Physica Scripta. Vol. 57, 488–494, 1998

A Powerful Soft X-ray Source for X-ray Lithography Based on Plasma Focusing

E. P. Bogolyubov,[5] V. D. Bochkov,[3] V. A. Veretennikov,[1] L. T. Vekhoreva,[4] V. A. Gribkov,[1] A. V. Dubrovskii,[1] Yu. P. Ivanov,[5] A. I. Isakov,[1] O. N. Krokhin,[1] P. Lee,[2] S. Lee,[2] V. Ya. Nikulin,[1] A. Serban,[2] P. V. Silin[1], X. Feng[2] and G. X. Zhang[2]

[1] Lebedev Physical Institute, Russian Academy of Sciences, Leninskiĭ Prospekt 53, 117924 Moscow, Russia
[2] Nanyang Technological University, 469 Bukit Timah Road, 259756 Singapore
[3] Scientific Production Corporation "Plasma", 390023 Ryazan, Russia
[4] St. Petersburg State Technical University, Politekhnicheskaya ul 29, 195251 St. Petersburg, Russia
[5] All-Russia Research Institute of Automatics, Moscow, Russia

Received July 11, 1997; accepted October 16, 1997

PACS Ref: 07.85.F

Abstract

A source of soft X-ray emission (9–14 Å) based on the miniature 15 kJ plasma focus was developed and tested. The X-ray emission was channelled along the chamber axis through an opening in the inner electrode (anode). A regime with a mean output of more than 100 J per discharge was found. At a discharge current of 280 kA and repetition rate of 3.5 Hz achieved by the device, its lifetime was estimated to be 10^7 commutations (about a year of continuous operation). A demonstration experiment on irradiation of an X-ray resist is discussed.

1. Introduction

Current progress in a number of areas of science and technology related to the study and manufacture of nanostructures (such as investigations of "wet" biological fabrics and nanoelectronics technology) is based on mastering the production of sources of radiation with wavelengths of the order of or shorter than 0.1 μm and the accompanying techniques for forming structures using this radiation. It is obvious that the most important sources are those with wavelengths shorter than the scale indicated. For such sources to be effectively used in nanophysics, they must satisfy a whole series of specific requirements; the most important of these are that their spectra be as monochromatic as possible and that the beams of radiation diverge as little as possible. It is clear that X-ray lasers would provide an ideal solution to this problem. Work on such lasers, however, is still in a rudimentary stage, and it is too early to count on rapid progress in this area to provide a technologically and commercially viable installation. Fortunately, there are other powerful sources of soft X-ray radiation with parameters that are fully satisfactory for the requirements of some areas of science and technology. Unsolved problems concerning these sources are the reproducability of the soft X-ray pulses, and the high rate of operation and the lifetime of installations.

Investigations are being carried out along two main directions, using proximity and projection X-ray techniques. In the first case, the optimum wavelength is very short (usually of the order of 10 Å), in order to avoid diffraction effects without simultaneously decreasing the gap between the object and detector (resist) to technologically unacceptable values (usually several micrometers). In the second case, longer wavelength radiation is used (of the order of 100 Å), so that it is possible to use X-ray optics based on multilayer reflecting mirrors and phase-zone plates. After fifteen years of work in this field, only three sources appear to be promising for the applications indicated above: sources based on synchrotron radiation from relativistic electrons, sources based on laser produced plasma, and pinch-plasma sources. The first tupe of source requires relatively expensive accelerators, in particular, steppers (due to the necessity that they be positioned vertically); the second has a low efficiency and a number of technological deficiencies. In connection with this, recent work [1, 2] in this field has given more and more attention to point sources of soft quasi-monochromatic X-ray emission based on the z-pinch. Because of their constructional properties, "plasma focus" installations are the best for such sources [1–4]. In light of the factors indicated above, we concentrated our attention on creating a soft X-ray source based on a plasma focus pinch device.

We thus developed and tested a plasma-focus soft X-ray source (9–14 Å). The main energy storage devices in our setup were four KMK-30-8 high-voltage impulsive capacitors [9] with total energy storage capacity to 15 kJ. The commutators were four EVOLYUTA-1 [5, 6] thyratrons with cold cathodes, each designed for commutating up to 150 kA. One of the main problems that had to be solved during the development of the facility was providing a long lifetime. Our solution was based on selecting the most current elements and systems and lowering their operational parameters in comparison to the maximum allowable values. At the discharge current of 280 kA and repetition rate of 3.5 Hz achieved by our device, we estimate its lifetime to be 10^7 commutations (about a year of continuous operation). The soft X-ray source itself was a miniature plasma-focus chamber filled with neon at a pressure of 10–25 mbar. The X-ray emission was channelled along the chamber axis through an opening in the inner electrode (anode). The radiation was recorded using PIN diodes. Roughly 20 000 discharges were produced on the four-capacitor device. We searched for an optimal operational regime and adjusted the shape and dimensions of the plasma-focus chamber electrodes to optimize the device for the absolute X-ray radiation output. We found a regime

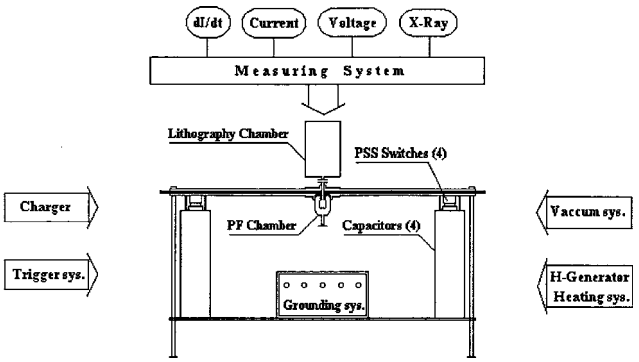

Fig. 1. The schematic diagram of the basic device

with a mean output of more than 100 J per discharge. We conducted a demonstration experiment on irradiation of an X-ray resist with characteristic dimensions for its element of about 5 μm.

2. General description of the device's construction

Our device consists of the following constructional elements and systems:

- energy storage provided by four capacitors;
- a discharge device;
- four pseudo-spark gaps, commutating the capacitor discharge to the discharge chamber;
- four heating systems for the commutator hydrogen generators;
- a four-channel system for ignition of the switches based on a spark gap;
- a pulse generator that sets off the ignition system for the pseudo-spark gaps;
- high-voltage buses and a collector;
- a "plasma-focus" discharge chamber;
- a vacuum pumping system;
- a system for filling the discharge chamber with working gas, with control of the final pressure;
- an output channel for the X-ray radiation, permitting investigations of the parameters of the radiation and irradiation of X-ray photo-resists;
- a discharge system and safety system;
- a set of diagnostic methods and recording devices.

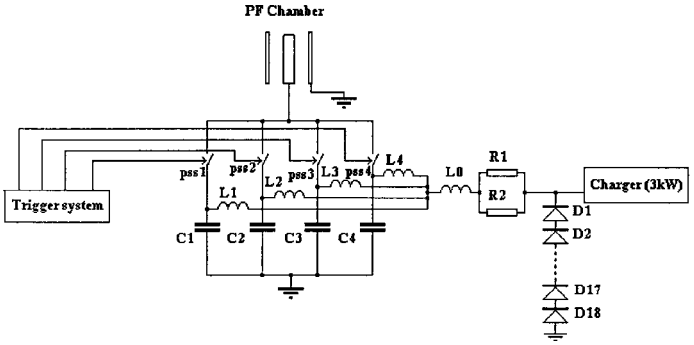

Fig. 2. The main electric circuit for the basic device.

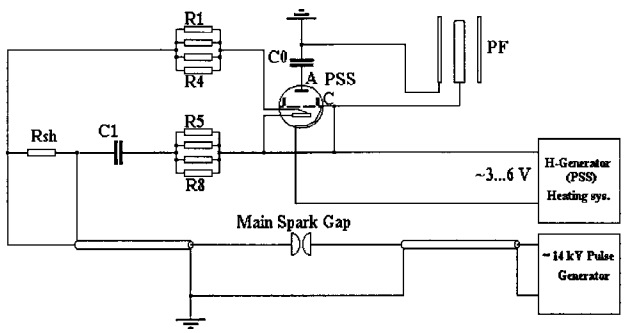

Fig. 3. The main circuit of the ignition system.

Figure 1 shows a schematic diagram of the device. The four high-voltage capacitors are located at the four corners of a rectangle with sides 1050 × 990 mm^2; a commutator is installed directly on each capacitor. The device uses a discharge circuit with a grounded plus. The plasma focus chamber is placed in the current collector, which is made of brass with an application of kaprolon nylon as an insulator, so that the vacuum system connects to it from below (Fig. 1). The output channel for the X-ray radiation is directed upward, where a chamber for irradiation of an X-ray resist with X-ray dosimeters is mounted, with its own vacuum pumping system. Collet clamps are used to hold the plasma focus chamber in the current collector. Figure 2 shows the electric circuit for the device. The main circuit for the ignition system, which will be described in more detail, is presented in Fig. 3.

3. The high-voltage capacitors

The high-voltage impulsive capacitors used for energy storage were developed at the St. Petersburg State Technical University especially for our device. They have been given the KMK-30-8 (low-inductance castor capacitors, voltage 30 kV, capacitance 8 μF, with design inductance 10 nH). The special construction of the capacitor leads ensures not only small inductance of the capacitor itself, but also provides for a low-inductance connection for the commutator. This was possible because the construction elements for the mating – the capacitor and commutator – were made mutually compatible by the engineers during the planning of the device. The system of capacitor leads and prefabricated buses has enhanced thermal and dynamical stability, which makes it possible to achieve a nominal current value of up to 350 kA (on one capacitor) during a discharge to a low-inductance load. The use of polymer capacitor plates and capacitor papers with enhanced electrical strength allowed us to substantially decrease the thickness of the dielectric section and weaken the edge of the foil. The capacitor weight is 70 kg and its dimensions are 240 × 270 × 680 mm^3.

Due to the use of an optimal structure for the combined insulation, the design capacitor lifetime for nominal voltages is 10^6 discharges. The capacitor is intended to operate with aperiodic discharges at a repetition rate of up to 1 Hz. If the operational voltage is lowered, it is possible to increase the pulse repetition rate, and the capacitor lifetime increases according to the power law dependence $(U/U_0)^6$. For example, at voltages that are half the nominal voltage, i.e., about 15 kV, the expected increase in the lifetime is two orders of magnitude. In other words, the capacitor lifetime at a voltage $U = U_{nom}/2$ should be of the order of 10^8 discharges, which should correspond to a time interval of 3 years for continuous operation with a repetition rate of 3 Hz.

We note, however, that the conditions for aperiodic discharge are important when estimating the capacitor lifetime. In the device described, the discharge has the form of decaying oscillations which are not aperiodic). In this case, the capacitor lifetime is determined by some effective voltage, made up of the charging voltages and the amplitude of the second half-wave of the discharge voltage (the maximum polarity reversal voltage). The operational charging voltage in our experiment was 12 kV; as can be seen from the voltage oscillogram (Fig. 8), the polarity reversal voltage was 70% of the charging voltage, or 8 kV. Thus, we should estimate the lifetime of the capacitor for these conditions using an effective voltage $U_{\text{eff}} = 20\,\text{kV}$. The lifetime of our high-voltage KMK-30-8 capacitor in this case is slightly higher than 10^7 discharges, i.e., about a year of continuous operation.

4. The commutator

To commutate the impulsive energy to a load in the device, we used a thyratron with a cold cathode, also called a pseudo-spark gap or low pressure spark gap. We used an EVOLYUTA-1 [5–7] low pressure spark gap with maximum anode voltage 25 kV, maximum anode current amplitude 150 kA, maximum discharge frequency 50 Hz, and minimum operating age (lifetime) in terms of the total charge commutated of more than 5×10^5 C.

Figure 4 shows the external appearance and construction of the EVOLYUTA-1 pseudo-spark gap. The low pressure spark gap is filled with gas at a pressure of 0.01–0.8 Torr. For currents to approximately several kiloamperes and pulse durations to 1 μs, initiation and development of the discharge, as well as the achievement of the conducting phase, occur in a gas-filled medium; for larger currents and pulse durations – as in vacuum conditions – they occur in vapours of material from the hard metallic cathode. The ballast volume is open to the inter-electrode space via four openings with diameter 3–4 mm, located in a circle with a 40 mm circumference.

Studies of the low pressure spark gap showed that the rapid decrease of the electrical strength of the spark gap caused by the appearance of dielectric films of ceramic material on the sides of the cathode surface had a very large influence on its longevity. We were able to fully eliminate this effect using a special, so-called re-entrance arrangement of the main electrodes, a screening system, and special dielectric covering for the inner surface of the ceramic insulator to protect it from the action of the arc discharge.

The main role in increasing the lifetime indicators of the low pressure spark gap is played by the special construction

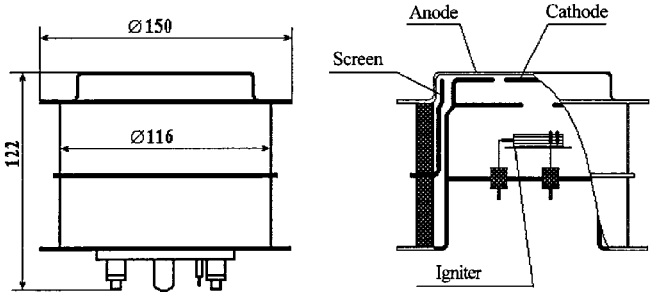

Fig. 4. The external appearance and construction of the EVOLYUTA-1 pseudo-spark gap.

of the cathode. Erosion of the cathode was decreased using a "sandwich" structure, with layers of materials with different values for their heat sublimation. The uppermost layer, facing the anode, has the minimum value, and layers of materials with increasingly larger heats of sublimation are arranged deeper.

This cathode operates as follows. In the initial period, as is usual, the discharge causes a local destruction of some part of the working surface around the circumference of the cathode opening. The low-melting material vaporizes from this area, with subsequent exposure of the underlying layer of high-melting material, leading to a worsening of the conditions for vaporization. As a result, a deficit of charge carriers arises, and the discharge voltage is decreased. Since it is energetically favourable for the discharge to burn in the low-melting material, a situation is created in which the discharge channel is shifted to the neighbouring section of the working surface, where the layer of low-melting material has not been depleted. With time, nearly the entire surface layer of low-melting material is depleted in this way. After this, the depletion of the deeper, second layer begins. In principle, if there are several layers of different materials, this process is repeated for each, leading to the destruction of increasingly deeper layers.

Thus, during the operation of the spark gap, this "sandwich" structure automatically regulates the more even, complete, and sequential depletion of the cathode, thereby increasing its longevity. Making the working surface of the cathode from low-melting material creates conditions that lower the energy required to maintain the burning of the arc discharge and ensure that the current pulse has a smooth shape, without breaks or sharp oscillations.

In the ignition node, we used a cylindrical igniter of polycrystalline boron carbide-nitride mounted on a ceramic plate. One of the ignition electrodes was a pin at one end of the cylinder; the second electrode, which is in the shape of a copper wire spiral, bends around the middle part of the lateral surface of the cylinder. Due to its polycrystalline structure, the igniter has a rough surface with many protuberances, which form a large number of contact points with the winds of the copper wire, each with its transition resistance. When the ignition voltage is delivered, a spark forms at one of the points of contact, where the conditions for energy release are optimal; if the ignition energy is sufficient, this spark causes the development of a discharge spanning the gaseous space above the surface of the igniter between the electrodes. The field formed between the cathode and igniter causes electrons from the resulting discharge plasma to be injected through the cathode openings into the space between the cathode and anode of the low pressure spark gap, igniting the main discharge.

In this process, sparks are created at various points of the igniter. The igniter material and the copper wires gradually vaporize. The service time for this type of construction exceeds 5×10^6 pulses for ignition parameters $U_{\text{tr}} = 2\,\text{kV}$, $I_{\text{tr}} = 100\,\text{A}$, and $C_{\text{tr}} = 0.2\,\mu\text{F}$. During the working regime of the ignition system, about 0.4 J of energy is released in the igniter. In order for the operation of several spark gaps to be highly synchronous (see below), we used nanosecond ignition pulses with energy two orders of magnitude lower than recommended. No deviations from the usual working regime of the low pressure spark gap were noted. This mode

of operation should increase the expected lifetime of the ignition system of the low pressure spark gap. The resistance of the igniter R_{tr} was usually from 10 Ohm to several kOhm.

A variable voltage from 3–6 V was applied to the hydrogen generator (not shown in Figure 4); the specific value of this voltage was carefully chosen for each low pressure spark gap in a series of "practice" starts, and must be controlled during its subsequent use, since it determines the operational pressure of the gas in the interelectrode space, and consequently the electric strength of the discharge. Experience showed, however, that after starting from different voltages for each of the four low pressure spark gaps, after about 100 starts, all four pseudo-spark gaps began to operate very regularly at a single voltage, equal to 5 V. One of the leads of the hydrogen generator is connected to the cathode of the low pressure spark gap. This required the use of isolation transformers (designed for 100 kV) in the power chain for the hydrogen generator for each of the four low pressure spark gaps. The initial winding of the transformer was fed from its thyristor circuit, ensuring smooth regulation of the hydrogen generator voltage.

It should be noted that the construction for the low pressure spark gap we have described makes it possible to use it in a periodic operating regime, i.e., when the first and second half-periods of the discharge current are equal in amplitude. As we already noted the discharge has the character of a decaying oscillation; in our device, this does not affect the longevity of the low pressure spark gap in any way. To estimate the expected lifetime of the low pressure spark gap in the experiment described, we can begin with the fact that roughly 0.15 C of electric charge is transferred through it in a single discharge. Considering the passport value for the maximum total charge transfer of 5×10^5 C, we estimate that the lifetime of the spark gap will be 3×10^6 discharges.

5. System for starting and synchronization of the EVOLYUTA-1 pseudo-spark gap

To achieve high reproducability (stability) of the parameters for the X-ray radiation obtained in a plasma focus installation, the time scatter for the operation of the high-precision EVOLYUTA-1 spark gaps used for the commutating must be minimal (not more than several nanoseconds). This requirement is also made by safety considerations – when the scatter in the starts of the discharges for each of the capacitors is so small, it is not possible to have a situation where the discharge of the capacitor that discharged first goes not to the plasma focus, but instead to another "late" capacitor.

It was not possible to satisfy this condition using the starting circuit for the low pressure spark gaps proposed by their developers, since it provided a starting pulse front of 0.5 μs. We therefore developed a series of other circuits. The best results were obtained when we used a generator in which a square-wave voltage impulse is formed using a coaxial cable and high-pressure (1–5 atm) spark gap. The main starting circuit is shown in Fig. 3. One four-channel gas spark gap and, correspondingly, four charge and discharge cables, each of length 6 meters, were used (one channel is depicted in Fig. 1. Thus, the system made it possible to obtain high voltage (4–5 kV) impulses with duration $t = 21/V_f$ where V_f is the velocity of propagation of the electromagnetic wave in the cable and l is the cable length. The duration of the leading edge of the impulse is determined by the inductance of the spark gap and the discharge space in it. In our case, the leading edge was about 6 ns and the impulse duration was 60 ns.

When developing this circuit, we tested both three-electrode and two-electrode gas spark gaps. In the first case, the third electrode, located between the two main electrodes, acted to initiate (ignite) the discharge, while in the second case, the circuit worked in a "self-breakdown" regime. In order to ensure stable, uninterrupted operation of the system in a Hertz regime, we used the two-electrode spark gap. The decrease in the instability of the time of breakdown of the gas gap was due to the fact that the spark gap was tuned to the self-breakdown long before the maximum discharge voltage was achieved (in our case at 6 kV as opposed to the maximum discharge voltage of 15 kV).

Operation of the spark gap in a Hertz repetition regime was provided by the impulse charge circuit of the charge cables (Fig. 3). In order to have synchronization with the diagnostic spark gap apparatus, another channel was added, i.e., another charge and discharge cable were used. The ignition impulse was applied to the controlling electrode of the psudo-spark gap through a KVI-3 S3 isolation capacitor. A shunting resistance R_{sh} installed in one of the channels was used to remove the charge from the cables.

6. The plasma focus chamber

The basis of our experiments was a miniature plasma focus chamber, initially developed as a neutron source using deuterium as the working gas. This chamber provided up to 10^8 fast neutrons per discharge for 3 kJ of energy stored in the storage device. During a low-inductance discharge, a short-lived (10–100 ns) hot (T_e and T_i to 1 keV), dense (to 10^{19} particles per cm^3) plasma formed on the axis of the plasma focus chamber; during the time it exists, this plasma is a source of neutrons and X-ray radiation over a wide spectrum (this formation is called the "plasma focus"). The chamber electrodes are prepared of especially pure unoxidized copper. Special technology is used during the assembly of the chamber, such as welding of the metal by an electron beam; spray application of a metallic layer onto the ceramic surface, so as to make it suitable for subsequent vacuum welding with metallic components; and so forth. Very important distinguishing properties of the chamber are the absence of any rubber seals and the matching of the joining materials in their coefficients of thermal expansion.

In order to outfit the chamber for X-ray lithography, it was necessary to change the construction of its inner electrode so that we could output the X-ray radiation through it, with subsequent channelling to an irradiation target with an angular aperture of 5 degrees. In order to increase the intensity of the radiation extracted from the plasma focus chamber at the required soft X-ray wavelengths (9–14 Å) required for X-ray lithography, we used neon as the working gas (Ne IX and Ne X lines). Exchanging the deuterium gas usually used in the chamber with neon required some changes in the chamber construction to ensure that the electrical and dynamical parameters of the discharge

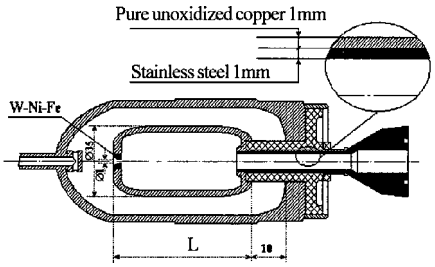

Fig. 5. The late version of the plasma focus chamber.

were consistent. In particular, we varied the length of the inner electrode L (Fig. 5) in the range from 35 mm to 54 mm (the optimal length proved to be about 45 mm).

For each inner electrode length, we selected the initial pressure for the working gas filling the chamber. Our selection criteria were that the time of formation of the plasma focus should coincide with the beginning of the decay of the discharge current curve, and also that the "singularities" in the current oscillogram be deep. The transition to a full-scale experiment with four capacitors required substantial increase in the mechanical strength of the X-ray output channel, since the magnetic field corresponding to the increased current for this case proved to be so large that its pressure crushed the channel after 30–50 "firings". We were able to eliminate this deficiency by filling the inner electrode with a two-part output channel: coaxial tubes of copper and stainless steel welded together in the outer part of the chamber. In its final form, the inner electrode of the plasma focus chamber has an insert made of a high-melting W–Ni–Fe allow with an opening of diameter 1 mm, which, in addition to increasing the longevity of the chamber, will make it possible in future experiments to use differential vacuum pumping for the volume of the plasma focus chamber itself and the X-ray lithography chamber. This is very important, in view of the large absorption coefficient of gaseous neon in the working wavelength range for X-ray lithography. One of the late versions of the plasma focus chamber is schematically depicted in Fig. 5. As can be seen from this figure, the plasma focus chamber is neither a Filippov- nor a Mather-type chamber [3, 4], but rather, the electrode configuration places it somewhere between them. A chamber of this construction makes it possible to irradiate a $(27 \times 27)\,\mathrm{mm}^2$ square area 430 mm from the plasma focus with soft X-ray radiation.

7. Experiment with a single capacitor

This experiment preceded the full-scale tests using the device described above, and was done to verify the performance of the elements used. We used a single high-voltage capacitor as the energy storage device; this capacitor had the same parameters as described above, but was an earlier version made by the same producer, and therefore differed in its larger dimensions and mass. The ignition of the low pressure spark gap was carried out using the circuit developed by its manufacturer (the recommended ignition parameters are presented above).

One significant way in which the preliminary experiment differed from the main one (apart from scale) was the use of a charging circuit with a negative inner plasma focus electrode and, accordingly, a positive outer electrode (the housing of the chamber). It is known that when a plasma focus chamber is used as a generator of neutrons or hard X-ray radiation, it is important that its inner electrode be the anode. Many years of study of the plasma focus phenomenon have shown that precisely in this case there are extinction phenomena when the current is pinched, which lead to the efficient acceleration of charged particles in the plasma, and consequently to the generation of hard radiation. In order to obtain soft X-ray radiation from the plasma focus in the form of Bremsstrahlung and line radiation of the hot neon plasma, it was not necessary to achieve the conditions under which current extinction phenomena and acceleration of charged particle fluxes would be observed. In this sense, the question of the electrode polarity lost its relevance. Nonetheless, we decided to use the traditional plasma focus electrode polarity for the full-scale device, and to output the radiation through a channel in the inner – positive – electrode. This decision to output the radiation through the anode was dictated by the fact that during the formation of the plasma focus during the discharge, there is a powerful cumulative plasma jet (and flux of accelerated ions, when there is particle acceleration) directed toward the cathode. If the radiation is output through the cathode, which is easier in terms of construction, the problem arises of protecting the output diaphragms, beryllium filters, etc. from the destructive action of the plasma and ion jets. In addition, it is very desirable to differentially pump the working gas (neon) due to its large absorption coefficient for the working radiation (wavelength 9–14 Å). This pumping should begin as near the pinch as possible, which is difficult to realize if the radiation is output through the cathode. These problems do not arise if the output is through the anode. We should add, that, as noted earlier, the output channel in the full-scale device is located at the top of the chamber. This also eliminates the necessity to clean the output filter of macroparticles incident from the plasma focus zone, as is done, for example, by Sato *et al.* [8], for the case when the radiation is output below.

For the preliminary experiment with a single capacitor, however, the inner electrode of the plasma focus chamber was chosen to be the cathode. This was done to simplify the assembly of the device, which was primarily intended only to test the electrical systems. In fact, as will be seen, this choice confirmed the fact that plasma focus is more effective when the inner electrode is positive.

Figure 6 depicts the circuit for the preliminary experiment, in which about 5000 discharges were produced. In these experiments, the capacitor was charged to a voltage of 13–15 kV; the discharge current reached values of 110–

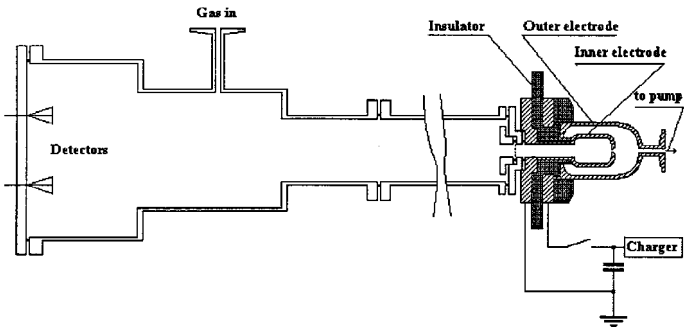

Fig. 6. The circuit of the preliminary experiment.

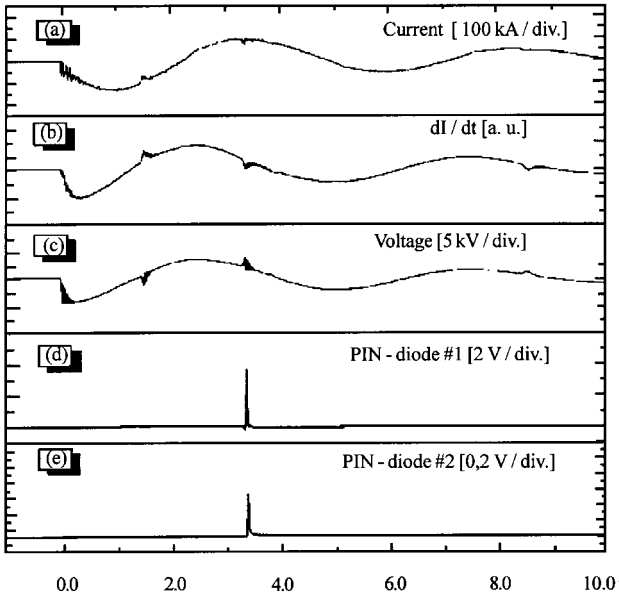

Fig. 7. Oscillograms of current (a), dI/dt- (b), voltage (c) and PIN-diode signals (d,e).

120 kA. The initial pressure of the working gas (neon) was varied over a wide range from 0.1–25 mbar; short (60 ns) impulses of X-ray radiation were recorded using PIN diodes in the pressure interval from 0.5–2.0 mbar (Fig. 7). It is interesting to note that, as can clearly be seen in the oscillogram in Fig. 7, the X-ray radiation is generated during the second half of the discharge current, i.e., at the time when the inner plasma focus chamber electrode takes on the function of the anode. This time corresponds to the so-called "singularities" in the curves for the current, voltage, and current derivative. In a number of cases, similar, "singularities" were also observed in the first half of the discharge (as, for example, in Fig. 7), but the observed X-ray impulse always corresponded to the "singularities" in the second half. Without embarking on a detailed discussion of this phenomenon, we emphasize that its main origin is the non-traditional polarity when the plasma focus chamber is commutated on in the charging chain. It is clear that this is also the reason why the intensity of the X-ray emission in this experiment was not very high (in the best discharges, it was not much greater than 0.5 J into the full solid angle).

The device worked in both a single and repetition regime. The range of repetition rates extended from 0.1–10 Hz. We conducted series of 100 or 200 discharges. The main result of this experiment was that it displayed the effectiveness of the selected circuit elements in the repetition regime. The highest temperature in this case is reached inside the plasma focus chamber itself. When we used only simple external water cooling of the chamber housing, its overheating was the main factor limiting the duration of a series. Because of the danger of excessive overheating of the inner plasma focus chamber electrode, the duration of the test series at a repetition rate of order 10 Hz did not exceed 50 discharges. It became clear from these experiments that in order to efficiently cool the chamber, it is most important to intensively remove heat from the inner electrode. Based on the results of the repetition regime experiments with a single capacitor, we decided to develop a new construction for the plasma focus chamber, allowing direct-flow cooling of its inner electrode.

8. The main experiment

The battery of four capacitors for the main experiment was charged to a voltage of 12 kV. The precise value of the battery's capacitance was 31.2 μF; thus, the energy stored before each discharge was 2.25 kJ. More than 20 000 discharges were produced on the device. After some adjustment, the ignition system provided synchronous operation of the four commutators, with a time scatter not exceeding 2 ns. The maximum of the discharge current in the first half was 280 kA. As we have already noted, the polarity when the charging circuit was turned on was such that the inner plasma focus chamber electrode was the anode. On oscillograms of the discharge current and voltage, we observe a well-defined "singularity" roughly at the place of maximum current virtually from the very first runs (Fig. 8). We varied the initial pressure of the working gas (neon) in the chamber in the range from 5–25 mbar. This enabled us to achieve the best agreement in the electrical and dynamical characteristics of the discharge for each version of the plasma focus chamber having a particular anode length. When the initial pressure was properly chosen, the "singularity" fell precisely at the maximum of the current oscillogram. The intensity of the X-ray radiation at this point was maximum.

The device operated in a single-start regime, and also in short series with various repetition rates. We used a charging device with limited power (3 kW) to charge the capacitor battery; in repetition regime experiments with the full capacitor battery, this enabled us to raise the discharge repetition rate only to 3.5 Hz. Compared to the single-capacitor experiment, the main experiment used a plasma focus chamber and current collector with a more massive input electrode, which should have provided more reliable electrical contact for the input and more intensive heat removal from the electrode. This did not provide a complete solution to the problem of overheating of the chamber during its operation in the repetition regime, however. This problem will apparently only be solved with the development of a plasma focus chamber with direct-flowing cooling.

The plasma focus soft X-ray radiation was recorded using two BRX 65 PIN diodes 62 cm from the plasma focus. The lithography chamber with the PIN diodes was separated from the plasma focus chamber by a beryllium filter with thickness 20 μm. Its volume was vacuum pumped by diffusion drift, so that the path from the filter to the detector was

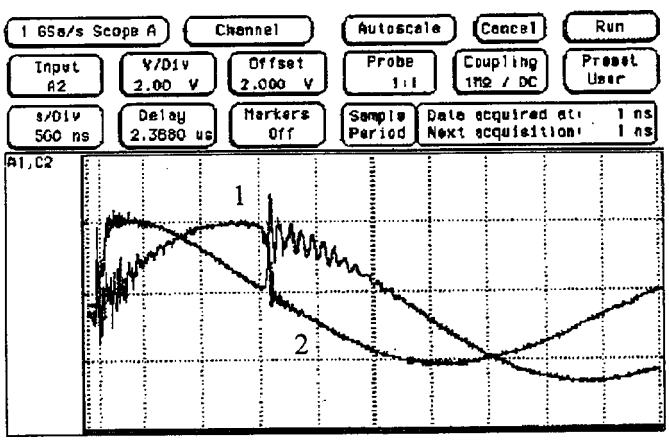

Fig. 8. Oscillograms of the discharge current (1) and voltage (2).

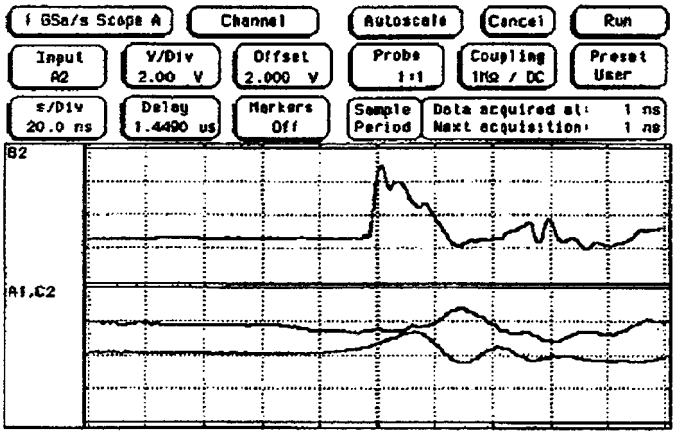

Fig. 9. The signals from the plasma focus X-ray bursts.

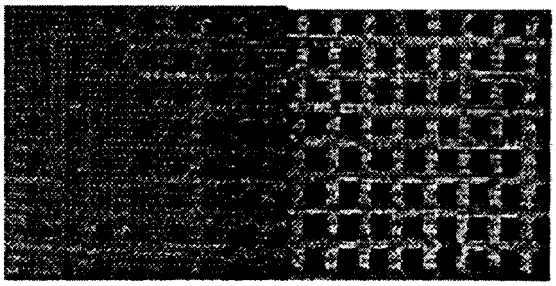

Fig. 10. The test exposure of the PMMA positive X-ray resists (a)-200 shots and (b)-400 shots.

transparent for the radiation of the required wavelength range (9–14 Å). The neon column inside the plasma focus chamber and the beryllium filter significantly weakened the radiation flux, however (this is a serious deficiency of this experiment, which will be corrected when differential pumping is used). Nevertheless, the detectors reliably detected the signals from the plasma focus X-ray bursts (See Fig. 9). Applying a two-channel method (with two different filters) made it possible to confidently determine whether the radiation detected was in the desired wavelength range. Dose calculations based on the experimental recordings using the transmission curves for neon and the materials used for the filters made it possible to determine the intensity of the recorded radiation. For the most advantageous version of the plasma focus chamber (with anode length 43 mm), this intensity was on average about 100 J per burst into the full solid angle. In order to be certain of the results obtained, we used PIN diodes, X-ray calorimeters, vacuum diodes, and RAR 2495 photofilms to measure the absolute soft X-ray output (the RAR 2495 photofilms were calibrated using impulsive lasers and laser plasma as a soft X-ray source, isotopic sources and a two-exposure method, and a synchrotron radiation beam from an accelerator of the Lebedev Physical Institute).

9. Conclusion

We conducted demonstration experiments on the irradiation of PMMA positive X-ray resists with sensitivity of the order of 1 J/cm^2 (see Fig. 10). These experiments will be described in detail in a future paper. Here, we present only their main result: test objects with characteristic dimensions 100 × 5 μm were successfully recorded with high contrast in the resists, which were located about 40 cm from the source, after about 100 bursts. In order to decrease the number of plasma focus bursts required for the resist exposures, and also to transfer the technique to spatial elements with dimensions of the order of 0.1 μm, it is necessary to use specialized X-ray resists with enhanced sensitivity at wavelengths 9–14 Å and to take special measures to suppress the smearing of the image by vibration of the device during the multiple irradiation of the resist.

Acknowledgements

We thank N. Kalachev (Lebedev Physical Institute) and V. Samarin (All-Russia Research Institute of Automatics) for help in the preparation of the experiments.

References

1. (a) Kato, J., Ochiai, I., Watanabe, Y. and Murayama, S., J. Vac. Sci. Technol. **B6**, 195 (1988); (b) Press release of SUSS Advanced Lithography, Inc. (Waterbury Center, Vermont 1997).
2. Prasad, R. R., Krishnan, M., Mangano, J., Greene, P. A. and Greene, N., SPIE–The International Society for Optical Engineering Proceedings of SPIE, **2194**, 120 (1994).
3. Filippov, N. V., Filippova, T. I. and Vinogradov, V. P., Nucl. Fusion Suppl. **2**, 577 (1962).
4. Mather, J. W., Phys. Fluids **3**, 134 (1960).
5. Bochkov, V. D., Zaydman, S. Sh., Sirota, E. I., Nechaev, A. G. and Kanareykina, N. A., Patent RF No 1792207, H01 T1/23, (1991).
6. Bochkov, V. D., Zaydman, S. Sh and Vosmerik, Yu. M., Patent RF No 1807798, H01 J17/44, (1990).
7. Bochkov, V. D., Korolev, Yu. D. and Shemyakin, I. A., Proc. Conf. Low Temperature Plasma Physics (Petrozavodsk 1995) p. 402.
8. Sato, T., Ochiai, T., Kato, Y. and Murayama, S., J. Appl. Phys. **69**, 385 (1991).
9. Bogolyubov, E. P., *et al.*, The Scientific and Technical Journal Appl. Phys. **1**, 35 (1997).